

ON THE MOVEMENT AND PREDICTION OF TRAVELING PLANETARY-SCALE WAVES

RAYMOND J. DELAND AND YEONG-JER LIN

New York University,* Bronx, N.Y.

ABSTRACT

Fluctuations of the planetary-scale waves, represented by spherical harmonics of the 500-mb. geopotential field, are statistically analyzed. A study is made of the prediction of these fluctuations from previous changes and using the non-divergent spherical vorticity equation.

1. INTRODUCTION

When numerical weather predictions were first computed using a planetary grid it was found that the largest or planetary-scale waves were computed to move rapidly westward at roughly 90° of longitude per day (Martin, [11]; Wolff, [13]). This produced a systematic error in the predictions, since the largest-scale waves do not move in this way. Cressman [3] introduced into the vorticity equation a "barotropic divergence" term, scaled so as to have its greatest effect at the largest scales. The magnitude of this term was empirically determined by the requirement that it reduce the mean-square error of the predictions as far as could be done by this means.

Recent observations of the planetary-scale waves at 500 mb. (Deland, [4, 5]; Eliassen and Machenhauer, [7]) have suggested that the fluctuations in position and amplitude of the waves are due to the simultaneous presence of a stationary and a traveling component. In the case of wave number 1, in middle-latitudes in winter, the stationary component has its maximum height over Europe and minimum height over the North Pacific corresponding to the long-term average. The traveling component, of somewhat smaller magnitude than the stationary one, moves westward at speeds variously estimated at 40° to 70° longitude per day.

The previously reported westward wave-speeds are, for the waves of largest scale, significantly less than those corresponding to the non-divergent vorticity equation (Rossby and collaborators [12], Haurwitz [9]). This suggests that a divergence term like that of Rossby and collaborators [12] is necessary for agreement between observed and calculated wave-speeds.

We have investigated the possibility of predicting the fluctuations of the planetary-scale waves, by statistically analyzing the fluctuations of the largest-scale spherical

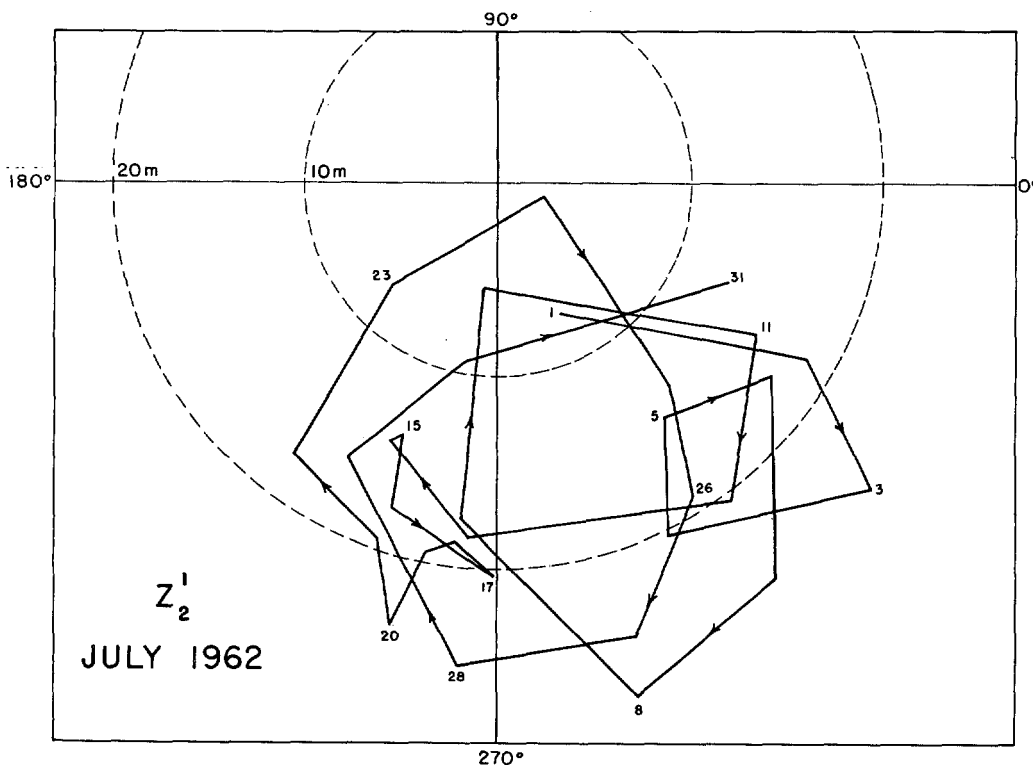
harmonics of the geopotential field. In this paper we present results of correlating the fluctuations (1) with the previous day's change and with fluctuations of other harmonics, and (2) with changes predicted from the barotropic vorticity equation, including non-linear interactions with the other large-scale waves. The first, autocorrelation, analysis was undertaken in response to the subjective observation that there are regularities in the fluctuations which do not fit the simple Rossby-wave model, but which could be useful for prediction. The second procedure provides a partial answer to the question: how well can we predict the fluctuations of the largest-scale waves by means of the (barotropic) vorticity equation?

The geopotential field was analyzed because it was immediately available at the beginning of the investigation and because previous work had already shown that it exhibited the phenomenon of traveling planetary-scale waves. Whether analysis of the stream function derived from the balance equation, as has been done by Eliassen and Machenhauer [7], gives a clearer picture of the phenomenon has yet to be determined. The main fluctuations of geopotential and stream function take place in middle latitudes, while the distribution of the fields among the different degrees of spherical harmonics is strongly affected by the variations in lower latitudes, so the analysis of either height or stream function into spherical harmonics must be considered somewhat "unnatural". It is, however, a convenient, though not precise, way of distinguishing between different latitudinal scales, whichever field is analyzed.

2. DATA

The data consist of surface spherical-harmonic expansions of 500-mb. geopotential over the Northern Hemisphere north of about 20°N. , for 00 GMT on each day of January 1–February 28 and July 1–August 31, 1962. The expansions consisted of "odd" (antisymmetric about the equator) harmonics only.

*Contribution No. 45, Geophysical Sciences Laboratory, Department of Meteorology and Oceanography, New York University. This research has been supported by the Section on Atmospheric Sciences, National Science Foundation, NSF GP-3728 and GA-362.

FIGURE 1.— Z_2^1 for July 1962.

The height field for the Northern Hemisphere at a particular hour is expressed as the sum of the odd harmonics

$$Z(\lambda, \phi) = \sum_{m=1}^M \sum_{n=m+1}^{M+L} (Z_{n_c}^m \cos m\lambda + Z_{n_s}^m \sin m\lambda) P_n^m(\phi) \\ + \text{zonal harmonics}$$

where the sum includes only values of n for which $n-m$ is odd. λ is longitude and ϕ is latitude. m is longitudinal wave-number and $2(n-m)$ corresponds roughly to wave-number in the latitudinal direction: the latitudinal scale decreases as n increases. For a given harmonic (m, n) , $Z_{n_c}^m$ and $Z_{n_s}^m$ are constant, and may be referred to as the magnitudes of the "cosine" and "sine" components of the particular harmonic. $P_n^m(\phi)$ is the associated Legendre function of the first kind.

3. MOVEMENT OF TRAVELING PLANETARY-SCALE WAVES

In this paper, we are concerned with the behavior of the largest scales only, as given by $m=1, 2$, and 3 and $n-m=1, 3$, and 5 .

The two components $Z_{n_c}^m$ and $Z_{n_s}^m$ constitute a vector amplitude Z_n^m , equivalent to scalar amplitude and phase, or the "complex amplitude" if complex exponentials are used. When the vector amplitude Z_n^m of a planetary-scale wave is plotted on a polar diagram for successive days as in figures 1 and 2, the plotted point describes a characteristic clockwise circular path. This behavior is

sketched in figure 3. The circular motion is interpreted (Deland [4]) as being due to a clockwise rotating vector, representing a westward-traveling component as also suggested by Eliassen and Machenhauer [7].

An interesting feature of the clockwise rotation is that it is often faster, corresponding to faster-moving waves, for smaller fluctuations. Although not apparent in figures 1 and 2 this behavior is evident on many plots of the waves (cf. Deland [4, 5]), especially those for Z_2^1 . The relation of speed to amplitude has not yet been quantitatively determined.

The fluctuations of Z_4^1 , in figure 2 (for August 1962) appear to be correlated with the simultaneous fluctuations of Z_2^1 plotted in figure 1. The fluctuations of Z_4^1 appear to be the sum of a slow clockwise motion and a faster clockwise motion in phase with the rotation of (1, 2).

COMPUTATIONS

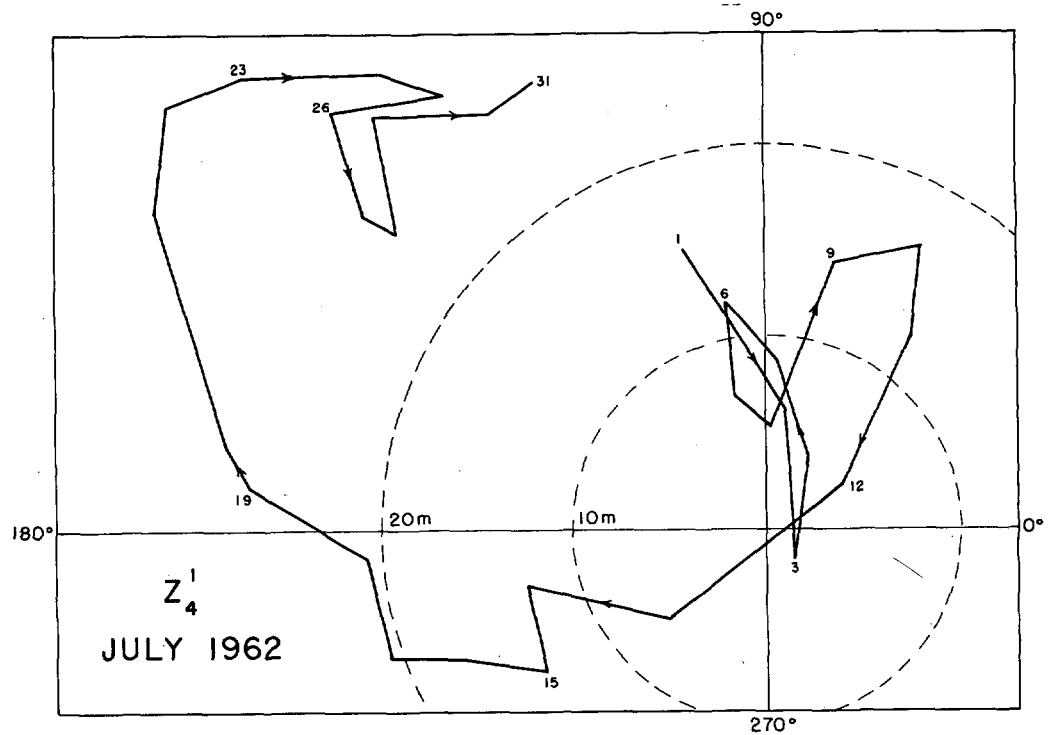
The rotation of the wave-vectors, corresponding to propagation of the traveling waves, and the relation between the waves of the same longitudinal wave-number m but different degree n , are both analyzed by computing least-squares vector regressions (Ellison [8], Anderson [1]).

The regressions are of the form

$$(\Delta X'_c, \Delta X'_s) = \begin{pmatrix} B_{11} & B_{12} \\ B_{21} & B_{22} \end{pmatrix} \begin{pmatrix} \Delta Y'_c \\ \Delta Y'_s \end{pmatrix}$$

and

$$(\Delta X'_c, \Delta X'_s) = \begin{pmatrix} C_{11} & C_{12} \\ C_{21} & C_{22} \end{pmatrix} \begin{pmatrix} \Delta Y'_c \\ \Delta Y'_s \end{pmatrix} + \begin{pmatrix} D_{11} & D_{12} \\ D_{21} & D_{22} \end{pmatrix} \begin{pmatrix} \Delta Z'_c \\ \Delta Z'_s \end{pmatrix}$$

FIGURE 2.— Z_4^1 for July 1962.

where c and s refer to cosine and sine components and the primes refer to deviations from the sample mean. The multiplication of a vector by a tensor corresponds to ordinary matrix multiplication. The first type of regression has been used recently by Lenhart, Court, and Salmela [10]. Correlation coefficients corresponding to the regressions were computed, and are presented below. For the multiple regression, these are total correlation coefficients, the square root of the fraction of the variance of ΔX "explained" by regression on both of the other vectors. The square of the correlation coefficient is also tabulated in each case.

The following regressions were calculated

$$\Delta Z_{nJ}^m = [B] \Delta Z_{nJ-1}^m \quad (1)$$

$$\Delta Z_{n_1J}^m = [B] \Delta Z_{n_2J}^m \quad (2)$$

$$\Delta Z_{n_1J}^m = [C] \Delta Z_{n_1J-1}^m + [D] \Delta Z_{n_2J}^m \quad (3)$$

$$\Delta Z_{n_1J}^m = [E] \Delta Z_{n_1J-1}^m + [F] \Delta Z_{n_2J-1}^m \quad (4)$$

where ΔZ_{nJ}^m is the 24-hr. change in Z_n^m beginning on day J (see fig. 3). The regression and correlation results are presented in tables 1-4. The first, auto-regression, procedure is schematically shown in figure 3.

The average speed of propagation of the traveling planetary-scale waves is estimated from the regression coefficients as follows. If the relation between one day's change and the next were a constant rotation, correspond-

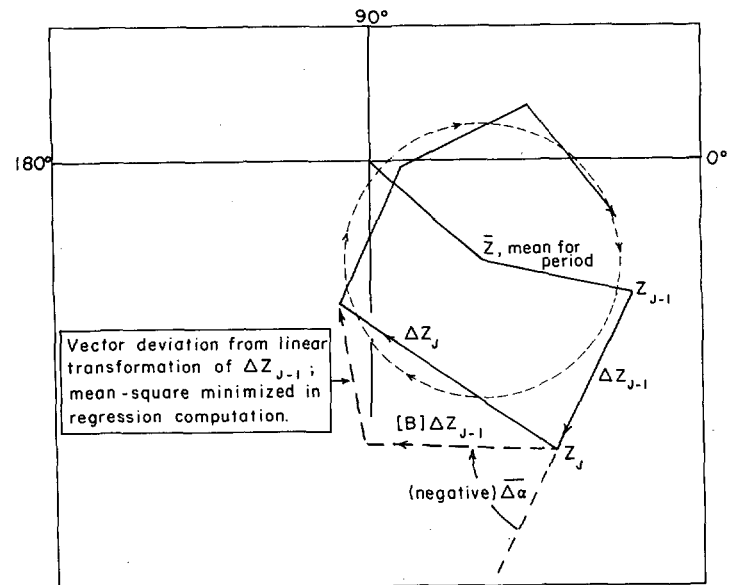


FIGURE 3.—Sketch of characteristic clockwise rotation and illustration of auto-regression procedure.

ing to a wave traveling at constant speed with constant amplitude, the regression tensor would be skew-symmetric, i.e., of the form

$$\begin{bmatrix} B_1 & B_2 \\ -B_2 & B_1 \end{bmatrix}, \text{ with } B_1^2 + B_2^2 = 1.$$

TABLE 1.—One day lag auto-regression-correlation of day-to-day changes. $\overline{\Delta\alpha}$ is angular rate of change, $\Delta\lambda$ is corresponding longitudinal speed, E & M is speed computed by Eliassen and Machenhauer [7], R - H is Rossby-Haurwitz speed, X is divergence factor (equation (8)).

σ_s (meters)		$\Delta Z_{n,J}^m = [B]\Delta Z_{n,J-1}^m$										
		B_{11}	B_{12}	B_{21}	B_{22}	R_s	R_s^2	$\overline{\Delta\alpha}$	$\overline{\Delta\lambda}$	$\frac{E \& M}{\Delta\lambda}$	R - H	X
January-February												
1,2	12.6	0.26	0.59	-0.44	0.27	0.58	0.34	-63°	-63°	-70°	-109°	4.4
1,4	14.0	.27	.16	-.17	.55	.49	.24	-22°	-22°	-20°	-20°	.8
1,6	15.5	.23	-.03	.07	.60	.42	.18	+8°	+8°	..	-4°	..
2,3	10.5	.27	.36	-.26	.08	.37	.14	-61°	-30°	-40°	-48°	6.6
2,5	13.6	.29	.19	.21	.41	.43	.18	+1°	0°	-12°	-11°	..
2,7	14.0	.29	-.19	.32	.58	.44	.19	+37°	+18°	..	+1°	..
3,4	10.3	.12	.03	-.11	.23	.19	.04	-22°	-7°	-20°	-23°	42.7
3,6	12.2	.51	-.27	.47	.05	.61	.26	+53°	+18°	-8°	-4°	..
3,8	14.6	.12	-.44	.52	.09	.49	.24	+77°	+26°	..	+4°	..
July-August												
1,2	10.7	.20	.94	-.66	.16	.82	.67	-77°	-77°	-70°	-116°	3.0
1,4	6.3	.24	.23	-.11	.30	.33	.11	-32°	-32°	-20°	-31°	..
1,6	8.1	-.23	-.01	-.01	.29	.27	.07	0°	0°	..	-12°	..
2,3	7.4	.05	.46	-.61	.20	.56	.31	-77°	-38°	-40°	-55°	5.1
2,5	6.6	.26	.17	-.14	.35	.35	.12	-27°	-14°	-12°	-19°	10.4
2,7	6.2	.12	.02	.01	.34	.26	.07	-1°	0°	..	-8°	..
3,4	6.1	.07	.54	-.50	.30	.55	.30	-70°	-23°	-20°	-31°	6.2
3,6	6.6	.53	.23	-.24	.33	.52	.27	-29°	-10°	-8°	-12°	10.0
3,8	6.3	.21	-.08	.03	.38	.31	.10	+11°	+4°	..	-5°	..

TABLE 2.—Cross-correlation of changes for pairs of harmonics. $\overline{\Delta\varphi}$ is phase difference between two harmonics.

		$\Delta Z_{n,J}^m = [B]\Delta Z_{n,J}^m$													
		January-February							July-August						
		B_{11}	B_{12}	B_{21}	B_{22}	R_s	R_s^2	$\overline{\Delta\varphi}$	B_{11}	B_{12}	B_{21}	B_{22}	R_s	R_s^2	$\overline{\Delta\varphi}$
Z_2^1	Z_2^1	0.50	0.12	-0.19	0.43	0.53	0.28	-18°	0.63	-0.10	0.34	0.90	0.49	0.24	+16°
Z_2^2	Z_2^2	-.10	.23	-.16	.17	.29	.08	-----	-.58	-.05	.13	-.02	.34	.12	+163°
Z_4^1	Z_4^1	.47	-.15	.21	.63	.53	.28	+18°	.19	.15	.00	.38	.52	.27	-15°
Z_4^2	Z_4^2	.33	.06	-.12	.72	.64	.41	-----	.19	.02	.11	.45	.40	.16	+8°
Z_6^1	Z_6^1	-.04	-.11	.39	.31	.29	.08	-----	-.37	.08	.02	-.02	.37	.14	-172°
Z_6^2	Z_6^2	.48	.07	.24	.79	.64	.41	+7°	.41	.08	-.05	.50	.36	.13	-9°
Z_8^1	Z_8^1	.34	-.01	-.04	.33	.43	.19	-2°	.54	.05	.09	.55	.49	.24	+2°
Z_8^2	Z_8^2	-.03	.02	.00	.01	.03	.00	-----	-.08	.00	-.06	-.15	.10	.01	-165°
Z_{10}^1	Z_{10}^1	.62	.09	.13	.50	.44	-----	2°	.40	.07	.04	.46	.49	.24	-2°
Z_{10}^2	Z_{10}^2	.60	.11	-.08	.63	.64	.41	-5°	.33	.13	-.16	.46	.41	.17	-20°
Z_{12}^1	Z_{12}^1	-.05	.00	.02	.03	.03	.00	-----	-.05	-.03	.01	.01	.10	.01	+168°
Z_{12}^2	Z_{12}^2	.63	-.09	.09	.69	.65	.42	+8°	.28	-.16	.09	.41	.41	.17	+20°
Z_{14}^1	Z_{14}^1	.64	-.14	-.15	.33	.59	.34	-1°	.55	-.02	.15	.69	.68	.46	+8°
Z_{14}^2	Z_{14}^2	-.06	.11	.02	-.05	.12	.01	-----	-.06	-.25	-.10	-.31	.28	.08	+136°
Z_{16}^1	Z_{16}^1	.70	-.13	.05	.52	.55	.30	+8°	.76	.12	-.11	.68	.67	.45	-9°
Z_{16}^2	Z_{16}^2	.34	.35	-.04	.56	.64	.41	-25°	.40	-.29	.16	.23	.41	.17	+36°
Z_{18}^1	Z_{18}^1	-.07	.04	.15	-.11	.10	.01	-----	-.04	.24	-.15	-.26	.27	.07	-129°
Z_{18}^2	Z_{18}^2	.68	-.03	.39	.58	.62	.38	+18°	.43	.16	-.24	.14	.43	.18	-35°

With the assumption that the actual relation is the sum of such a rotation plus some additional non-rotational average "distortion", the problem of estimating the speed of propagation is reduced to that of estimating the skew-symmetric part of the regression, i.e., B_1 and B_2 . The skew-symmetric part of the regression tensor is given in terms of the computed components of the tensor by

$$\begin{bmatrix} \frac{B_{11}+B_{22}}{2} & \frac{B_{12}-B_{21}}{2} \\ -\frac{B_{12}-B_{21}}{2} & \frac{B_{11}+B_{22}}{2} \end{bmatrix}$$

The magnitude of the average angle of rotation from one day's change to the next is then given by

$$|\overline{\Delta\alpha}| = \arctan \frac{B_{21}-B_{12}}{B_{11}+B_{22}}$$

and its quadrant is easily determined from the skew-symmetric tensor. This angle is tabulated for each of the regressions in tables 1-4, with positive angles corresponding to clockwise rotation.

In view of the "tendency toward zero" of the regression coefficients when the correlation is low, evident in the computed values given in table 1, the question of bias in the estimates of $\Delta\alpha$ arises. It can be shown, using a

TABLE 3.—Double regression of changes for one harmonic on another harmonic and itself a day earlier. $\Delta\varphi$ is phase difference, $\Delta\lambda$ is equivalent longitude difference

$\Delta Z_{n,j}^m = [C]\Delta Z_{n,j-1}^m + [D]\Delta Z_{n,j}^m$

		January-February							July-August						
		C_{11} D_{11}	C_{12} D_{12}	C_{21} D_{21}	C_{22} D_{22}	R^2	$\overline{\Delta\varphi}$	$\overline{\Delta\lambda}$	C_{11} D_{11}	C_{12} D_{12}	C_{21} D_{21}	C_{22} D_{22}	R^2	$\overline{\Delta\varphi}$	$\overline{\Delta\lambda}$
Z_2^1	Z_2^1	0.18	0.54	-0.41	0.10	0.49	-74°	-74°	0.18	0.95	-0.55	0.04	0.74	-82°	-82°
	Z_4^1	.30	-.04	-.09	.40	-----	-4°	-4°	.00	-.13	.33	.57	-----	+39°	+39°
	Z_6^1	.24	.60	-.48	.17	.38	-69°	-69°	.19	.88	-.65	.26	.70	-73°	-73°
Z_2^1	Z_6^1	.07	.02	.03	.26	-----	-10°	-10°	-.15	.07	.26	.08	-----	+70°	+70°
	Z_4^1	.25	.08	.05	.45	.42	-11°	-11°	.10	.17	-.05	.36	.35	-26°	-26°
Z_4^1	Z_2^1	.45	-.12	.01	.52	-----	+10°	+10°	-.02	.35	-.05	.30	-----	-73°	-73°
	Z_4^1	.12	.20	-.25	.23	.48	-51°	-51°	.23	.27	-.09	.29	.26	-35°	-35°
	Z_6^1	.33	-.03	.01	.61	-----	+3°	+3°	.21	.05	.14	.40	-----	+9°	+9°
Z_6^1	Z_2^1	.23	-.03	.12	.44	.23	+13°	+13°	-.39	.00	.05	.04	.22	+171°	+171°
	Z_4^1	.01	-.11	.28	.29	-----	+54°	+54°	.35	.35	-.16	.16	-----	-45°	-45°
Z_6^1	Z_6^1	.24	-.11	.01	.24	.46	+14°	+14°	.34	.04	.09	.50	.21	+4°	+4°
	Z_8^1	.50	.08	.20	.69	-----	+6°	+6°	.17	-.37	-.10	.41	-----	+25°	+25°
Z_8^1	Z_2^1	.20	.37	-.26	.02	.30	-71°	-36°	-.05	.40	-.57	.08	.46	-88°	-44°
	Z_4^1	.32	-.06	.00	.31	-----	+5°	+2°	.46	-.07	.22	.38	-----	+19°	+10°
Z_6^1	Z_6^1	.30	-.08	.16	.11	.46	+30°	+10°	.40	.28	-.36	.33	-----	-41°	-14°
	Z_8^1	.36	.18	-.01	.44	-----	-13°	-4°	.26	-.28	.35	.23	-----	+53°	+18°
Z_8^1	Z_2^1	.13	-.44	.52	.07	.25	+79°	+26°	-.10	.26	-.02	.30	-----	-145°	-48°
	Z_4^1	.03	-.02	.13	-.12	-----	-60°	-20°	.69	-.42	-.65	.60	-----	-11°	-4°
Z_8^1	Z_6^1	-.01	-.50	.36	.00	.54	-89°	-30°	.40	.16	-.19	.06	-----	-37°	-12°
	Z_8^1	.70	.14	.36	.40	-----	+110°	+4°	.20	-.04	-.06	.59	-----	+22°	+7°
Z_8^1	Z_2^1	.27	.37	-.26	.07	.14	-61°	-30°	.05	.47	-.61	.21	.32	-76°	-38°
	Z_4^1	.00	-.03	.01	.01	-----	+77°	+38°	.04	-.03	.07	-.05	-----	+95°	+48°
Z_6^1	Z_6^1	.21	.13	.21	.42	.34	+7°	+4°	.35	.12	-.01	.40	.35	-11°	-6°
	Z_8^1	.52	.08	-.04	.48	-----	-7°	-4°	.13	.36	-.31	.36	-----	-54°	-27°
Z_6^1	Z_2^1	.17	.23	.23	.04	.48	-24°	-12°	.19	.24	-.20	.21	.25	-48°	-24°
	Z_4^1	.60	-.04	-.07	.54	-----	+5°	+2°	.34	.02	-.11	.42	-----	-10°	-5°
Z_8^1	Z_6^1	.30	-.19	.33	.39	.19	+37°	+18°	-.07	-.05	.02	-.09	.07	+113°	+56°
	Z_8^1	-.01	-.04	.00	-.05	-----	-33°	-16°	.13	.02	-.12	.31	-----	-17°	-8°
Z_8^1	Z_2^1	.18	-.20	.26	.14	.49	+55°	+27°	.25	-.21	-.10	.39	.23	+25°	+12°
	Z_4^1	.60	-.01	.05	.58	-----	+3°	+2°	.07	.04	.01	.30	-----	-6°	-3°
Z_4^1	Z_6^1	-.07	.14	-.15	.18	.38	-70°	-23°	-.12	.39	-.36	.10	-----	-88°	-29°
	Z_8^1	.67	-.13	-.09	.34	-----	+2°	+1°	.47	-.13	.22	.54	-----	+19°	+6°
Z_4^1	Z_4^1	.09	.04	-.10	.23	.05	-25°	-8°	.11	.52	-.51	.29	-----	-69°	-23°
	Z_6^1	-.07	.13	.03	-.03	-----	+46°	+15°	-.09	-.26	.22	-.14	-----	+116°	+37°
Z_6^1	Z_8^1	.39	-.27	.53	.00	.52	+64°	+31°	.62	.30	-.13	.61	-----	-19°	-6°
	Z_4^1	.64	-.06	-.04	.57	-----	+1°	0°	.58	.37	-.69	.05	-----	-59°	-20°

simple "rotation plus noise" model, that $\Delta\alpha$ is unbiased to the extent that it is not affected by the addition of random "noise" and/or an additional non-rotational component of the fluctuations.

For the regression of ΔZ_j on ΔZ_{j-1} the estimated angle corresponds to the phase speed of the waves; the spatial speed of propagation in degrees of longitude per day is then equal to the phase speed divided by longitudinal wave-number. The speeds of propagation are tabulated in tables 1, 3, and 4, with sign such that westward propagation corresponds to negative speeds, following the usual convention. For the cross-correlations between different degrees, the derived angle $\Delta\alpha$ corresponds to a phase shift between the rotating part of the two harmonics, one being ahead of the other. In this case a positive angle means that the "dependent" vector (on the left hand side of (2)) is on the average rotated clockwise from the "independent" vector (on the right hand side).

RESULTS

First considering the auto-regressions, ΔZ_j on ΔZ_{j-1} , it is apparent that the regression coefficients correspond to the simple rotation model to a varying extent. In the winter period only (1,2) and (1,4) and perhaps (2,3) show definite rotation. The rotation is considerably more apparent in the summer months, the regression coefficients for (1,2), (1,4), (2,5), and (3,6) all conforming to the skew-symmetric pattern quite closely, and the other two also doing so fairly well. It is also noticeable that the auto-correlation coefficients are also generally higher in the summer period.

In both periods the behavior of the largest-scale wave (1,2) is closest to the simple traveling wave model.

The estimated wave-speeds toward the west are in every case less in the winter than in the summer period, the difference ranging from 10° to 28° longitude per day. In view of the erratic form of some of the regression

TABLE 4.—Double regression of changes for one harmonic on both itself and another harmonic a day earlier. $\overline{\Delta\varphi}$ is phase difference, $\overline{\Delta\lambda}$ is equivalent longitude difference

		$\Delta Z_{n,j}^m = [E]\Delta Z_{n,j-1}^m + [F]\Delta Z_{n,j-2}^m$													
		January-February							July-August						
		E_{11} F_{11}	E_{12} F_{12}	E_{21} F_{21}	E_{22} F_{22}	R^2	$\overline{\Delta\varphi}$	$\overline{\Delta\lambda}$	E_{11} F_{11}	E_{12} F_{12}	E_{21} F_{21}	E_{22} F_{22}	R^2	$\overline{\Delta\varphi}$	$\overline{\Delta\lambda}$
Z_2^1	Z_2^1	0.30	0.66	-0.49	0.19	0.36	-67°	-67°	0.18	0.96	-0.67	0.16	0.69	-78°	-78°
	Z_4^1	-.03	-.11	.06	.13	-----	-----	-----	.11	-.08	.08	-.02	-----	-----	-----
	Z_6^1	.25	.57	-.46	.24	.35	-65°	-65°	.20	.94	-.63	.15	.69	-77°	-77°
Z_2^2	Z_2^1	-.10	.02	.02	.07	-----	-----	-----	-.01	.08	.08	-.13	-----	+1°	+1°
	Z_4^1	.24	.03	-.13	.50	.27	-12°	-12°	.20	.08	.03	.30	.19	-6°	-6°
	Z_6^1	.16	.26	-.03	.12	-----	-46°	-46°	-.03	.15	-.20	-.02	-----	+82°	+82°
Z_4^1	Z_4^1	.36	.26	-.29	.55	.27	-31°	-31°	.18	.34	-.19	.27	.19	-50°	-50°
	Z_6^1	-.13	-.11	.27	-.01	-----	-69°	-69°	.12	-.21	.21	.04	-----	+70°	+70°
	Z_2^1	.21	-.02	.12	.42	.16	+13°	+13°	.34	-.02	-.08	.30	.22	-5°	-5°
Z_6^1	Z_2^1	.23	-.26	.07	.30	-----	+32°	+32°	.10	-.42	.02	.03	-----	+74°	+74°
	Z_4^1	.08	-.06	.10	.30	.24	+24°	+24°	.27	.13	-.08	.32	.10	-19°	-19°
	Z_6^1	.44	.00	.00	.28	-----	0°	0°	-.07	-.31	-.01	-.06	-----	+67°	+67°
Z_2^2	Z_2^2	.21	.35	-.36	.07	.15	-68°	-34°	-.05	.44	-.59	.13	.34	-----	-----
	Z_4^2	.09	.11	.15	-.02	-----	-----	-----	.25	.02	-.08	.17	-----	-13°	-6°
	Z_6^2	.27	.36	-.26	.08	.15	-61°	-30°	.06	.47	-.61	.19	.32	-77°	-38°
Z_3^2	Z_2^2	-.04	.02	.10	.01	-----	-----	-----	.17	.02	.00	-.05	-----	-----	-----
	Z_4^2	.29	.23	.31	.43	.21	+6°	+3°	.19	.11	-.04	.33	.16	-16°	-8°
	Z_6^2	-.01	-.12	-.28	-.05	-----	-----	-----	.11	.11	-.21	.07	-----	-61°	-30°
Z_5^2	Z_2^2	.28	.35	.19	.24	.22	-17°	-8°	.22	.25	-.16	.38	.13	-34°	-17°
	Z_4^2	.06	-.22	.00	.24	-----	+36°	+18°	.19	-.13	.06	-.06	-----	-----	-----
	Z_6^2	.29	-.19	.32	.38	.20	+38°	+19°	.12	-.02	.02	.36	.12	+5°	+2°
Z_7^2	Z_2^2	.06	-.10	.05	.15	-----	+35°	+18°	.07	-.20	.13	.10	-----	+61°	+30°
	Z_4^2	.25	-.35	.23	.28	.23	+48°	+24°	.02	.11	-.03	.24	.14	-28°	-14°
	Z_6^2	.11	.24	.18	.14	-----	-14°	-7°	.20	-.24	.18	.19	-----	+48°	+24°
Z_4^3	Z_4^3	-.02	.06	-.14	.24	.05	-----	-----	-.10	.48	-.55	.16	.34	-----	-----
	Z_6^3	.20	-.01	.04	-.01	-----	-----	-----	.23	.05	.10	.19	-----	+6°	+2°
Z_3^3	Z_4^3	.09	.05	-.10	.22	.05	-26°	-9°	.03	.50	-.48	.31	.32	-71°	-24°
	Z_6^3	-.03	.16	.01	-.03	-----	-----	-----	-.08	-.23	.09	.12	-----	-----	-----
Z_6^3	Z_4^3	.55	-.31	.66	-.05	.28	-----	-----	.56	.02	-.11	.31	.30	-9°	-3°
	Z_6^3	-.04	.09	-.25	.21	-----	-----	-----	-.13	.31	-.25	.02	-----	-----	-----
Z_3^3	Z_6^3	.54	-.29	.36	.03	.28	+49°	+16°	.54	.28	-.29	.26	.31	-35°	-12°
	Z_2^3	-.07	.03	.13	.05	-----	-----	-----	-.12	-.17	.23	.23	-----	-----	-----
Z_8^3	Z_6^3	.14	-.46	.54	.05	.28	+80°	+27°	.23	-.07	.04	.45	.11	+10°	+3°
	Z_4^3	.13	-.15	.28	-.14	-----	-----	-----	.14	-.08	.18	.03	-----	+56°	+19°
Z_3^3	Z_8^3	-.04	-.49	.34	.01	.35	-----	-----	.09	.05	.04	.37	.16	-1°	0°
	Z_6^3	.45	-.18	.47	-.14	-----	-----	-----	.36	-.10	-.04	.03	-----	+8°	+3°

tensors, the consistency of the summer-winter speed differences may be partly coincidental.

Let us compare these results with those of Eliassen and Machenhauer [7] (which are for movement of the tendency field, but comparable) and Deland [5]. As shown in table 1, Eliassen and Machenhauer's results for January 1957 agree quite closely with ours, though, rather surprisingly, better with those for the summer period than those for the winter. Deland's [5] speeds for April 1961 are, on the other hand, all considerably greater algebraically, i.e., less westward than the others. Comparison of figure 1 with figure 1 of Deland [5] shows that the difference is not entirely due to the different methods of analysis: the rotation apparent in figure 1 (of this paper) for August 1962 is clearly more rapid on the average than that shown in the earlier paper for April 1961.

Considering now the results for the cross-correlations between different degrees, in table 2, we see that the relationship apparent in figures 1 and 2 shows up as a moderately high correlation of ΔZ_4^1 with ΔZ_2^1 in both sum-

mer (0.52) and winter (0.53). Correlations of similar magnitude appear for ΔZ_6^1 on ΔZ_4^1 (high correlation in winter, low in summer). ΔZ_5^2 on ΔZ_3^2 , and ΔZ_6^3 and ΔZ_4^3 , (0.67, in summer, 0.55 in winter). All "adjacent" pairs of harmonics, ΔZ_2^1 and ΔZ_4^1 , ΔZ_4^1 and ΔZ_6^1 , etc., are at least moderately well correlated and closely in phase, both in summer and winter. The correlations between ΔZ_2^1 and ΔZ_6^1 , ΔZ_3^2 and ΔZ_7^2 , ΔZ_4^3 and ΔZ_8^3 are small, but it is interesting that in summer the corresponding changes in these pairs are almost opposite in phase. This does not correspond to oppositely moving waves, a relationship that is excluded by the regression computation. The interpretation of this observation is postponed until after the results for the multiple regressions are presented.

The results for the multiple-regression correlations in table 3 show that the total correlations are in each case higher than for the correlations between pairs of vectors, presumably mainly because the independently varying parts of the vectors on the right hand side of equation (3) "explain" some of the variation of the dependent vector,

but also in part because of the decreased "degrees of freedom" of the computed coefficients. The interpretation of the partial regressions is complicated by the time lag between the dependent variable and one of the predictors (the predictand itself for previous day). In particular, the opposite phase of ΔZ_2^1 and ΔZ_6^1 etc., previously mentioned, is apparently masked by the fact that here we are regressing ΔZ_2^1 on the part of ΔZ_6^1 that is uncorrelated with ΔZ_2^1 for the previous day.

The calculated wave-speeds present a regular variation with scale, as can be seen from figure 4. The wave-speeds are considerably greater toward the east in winter than in summer, as has already been observed for the auto-correlations. The difference between winter and summer increases with decreasing scale, up to 25° to 30° of longitude per day for the smallest scales considered here.

According to calculations of Eliassen and Machenhauer [7], the difference between winter and summer speeds cannot be due to the difference in advection by the zonal wind, even allowing for the varying weighting of the latitudinal variation of the zonal wind for different harmonics. They have computed interactions with the zonal harmonics for December 1956–January 1957 (see their table 10) and it is apparent that not only are they small (except for (1,2), (2,3) and (3,4)) even in winter but they decrease with decreasing scale. It follows that the difference between the observed wave-speeds in summer and winter is considerably greater, for all but the largest scales, than can be explained by the non-divergent barotropic vorticity equation.

The relations between the different estimates of the speeds of the various waves is schematically represented in figures 5 and 6. Considering Z_2^1 in January–February, its actual westward speed from the auto-correlation calculation is 63°/day. Its fluctuations are correlated ($R=0.53$) with the slower fluctuations of Z_4^1 : when the speed of Z_2^1 is calculated holding Z_4^1 fixed (multiple regression), the estimated westward speed increases to 74°/day. ΔZ_2^1 is weakly correlated with ΔZ_6^1 : when this effect is removed (but the effect of ΔZ_4^1 remains), the estimated speed is 69° ($>63^\circ$, but $<74^\circ$). And similarly for the other harmonics; note especially the estimates of the speed of Z_4^1 : 22° "actual", 51° with Z_6^1 fixed but the interaction with the rapidly moving Z_2^1 present; 10° eastward when the effect of Z_2^1 is removed but the effect of the slower Z_6^1 is present. The observed speeds show a consistent pattern, in both the winter and summer periods. It is apparent that the speed estimates by simple auto-correlation are affected by the more rapid westward rotation correlated with the motion of the next lower degree. This effect is strongest in summer when the rotation of the lower-degree waves, Z_2^1 , Z_3^1 , and Z_4^1 , is more clearly defined.

The above results are consistent with a continuous spectrum of wave-speeds for each harmonic, which seems to be evident in the polar diagrams, as previously mentioned.

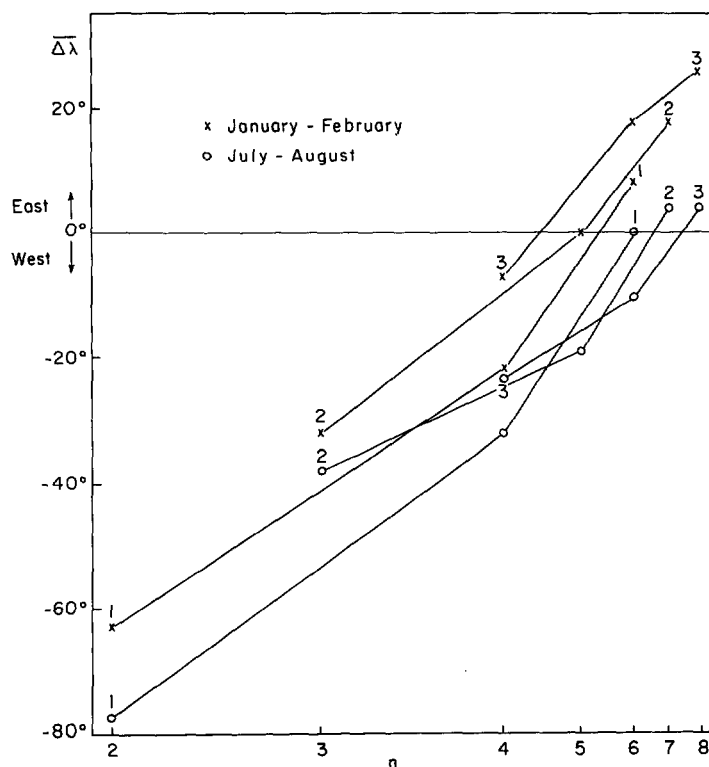


FIGURE 4.—Variation of wave-speed with scale. Abscissa is $1/n$, proportional to a representative linear scale. Points representing one longitudinal wave-number m are connected by straight lines with value of m indicated at points for lowest and highest degree n .

It appears that there are traveling waves present which are similar to spherical harmonics of the geopotential field, but not exactly the same. If we refer to the traveling wave that is mostly evident in ΔZ_2^1 as ϕ_2^1 , it appears that $\Delta \phi_2^1$, in summer at least, is made up mainly of Z_2^1 , some Z_4^1 , and a little negative Z_6^1 . Likewise for ϕ_3^1 and ϕ_4^1 . This raises the question of the form of the traveling waves, and in particular whether the use of spherical harmonics of a stream function derived from the balance equation would result in a better separation of different characteristic motions. This matter will be dealt with in a later article.

It is of interest to relate the mean speeds of the waves to the quasi-geostrophic barotropic vorticity equation, since even the largest-scale waves should be governed by it (Deland [6]). The barotropic vorticity equation can be written

$$\frac{\partial}{\partial t} (\nabla^2 z) + \mathbf{V} \cdot \nabla (\nabla^2 z) + \frac{2\Omega}{R^2} \frac{\partial z}{\partial \lambda} = 0 \quad (5)$$

where z is the geopotential height, R is the radius of the earth, and λ is longitude.

If a "barotropic-divergence" term, suggested by Rossby and collaborators [12] and further discussed by Charney

JANUARY - FEBRUARY

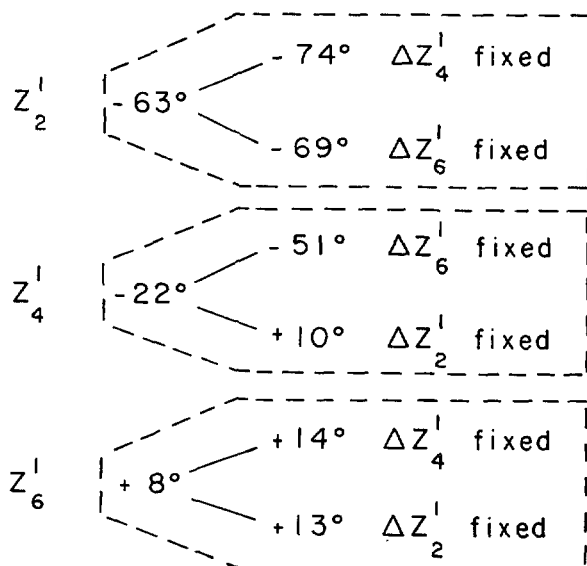


FIGURE 5.—Schematic diagram of different estimates of wave-speed, for $m=1$ in winter.

JULY - AUGUST

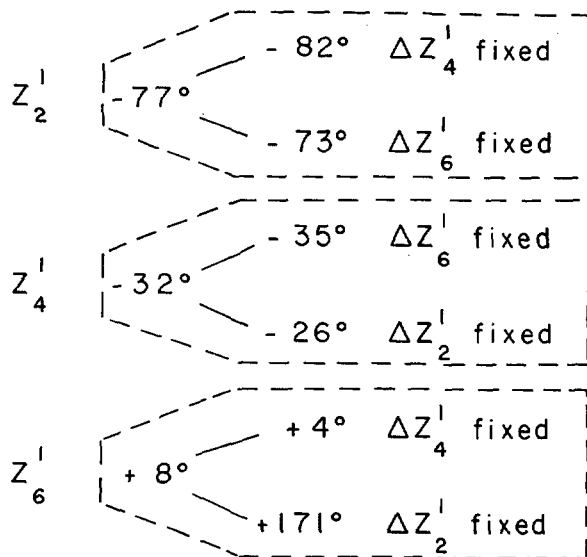


FIGURE 6.—Schematic diagram of different estimates of wave-speed, for $m=1$ in summer.

[2] and Cressman [3], is included, the vorticity equation becomes

$$\frac{\partial}{\partial t} (\nabla^2 z) + \mathbf{V} \cdot \nabla (\nabla^2 z) + \frac{2\Omega}{R^2} \frac{\partial z}{\partial \lambda} = \frac{\chi}{R^2} \frac{\partial z}{\partial t} \quad (6)$$

where χ is the divergence coefficient.

Equation (6) is identical to Eliassen and Machenhauer's equation (17), except that here we are using the geopotential instead of the stream function. The relation of χ to Cressman's coefficient μ is given by

$$\chi = \frac{f^2 R^2}{\bar{z}} \mu \approx 7.5\mu.$$

With the barotropic-divergence term included, the spherical-harmonic form of the vorticity equation is

$$\frac{d}{dt} Z_\gamma = -i \frac{n_\gamma(n_\gamma+1)}{n_\gamma(n_\gamma+1)+\chi} \left\{ \left[\frac{2(\Omega+\omega)}{n_\gamma(n_\gamma+1)} - \omega \right] m_\gamma Z_\gamma + \frac{g}{f} \Omega \sum_{\alpha, \beta} Z_\alpha Z_\beta I_{\gamma\alpha\beta} \right\} \quad (7)$$

in which γ identifies a particular harmonic of the geopotential height, of complex amplitude Z_γ ; m_γ and n_γ are the order (longitudinal wave-number) and degree of the particular harmonic; Ω is the rate of rotation of the earth; $\bar{\omega}$ is the average zonal wind, corresponding to the amplitude of the (0,1) harmonic, expressed as an angular velocity; Z_α and Z_β are the complex amplitude of other waves that affect Z_γ through the interaction coefficient $I_{\gamma\alpha\beta}$; χ is the divergence coefficient; and the other symbols have their usual meanings.

It is seen that the theoretical effect of the barotropic-divergence term is to reduce all wave-speeds (neglecting interactions with other waves) in the proportion $n_\gamma(n_\gamma+1)/[n_\gamma(n_\gamma+1)+\chi]$; i.e.,

$$\omega_{\text{obs}}/\omega_{R-H} = n_\gamma(n_\gamma+1)[n_\gamma(n_\gamma+1)+\chi]^{-1}.$$

We can thus estimate magnitudes of the coefficient χ that would correspond to the observed speeds. The mean Rossby-Haurwitz wave-speeds are calculated from the formula

$$\omega_{R-H} = \frac{2(\Omega+\omega)}{n_\gamma(n_\gamma+1)} - \bar{\omega}.$$

Thus the value of χ corresponding to the observed wave-speeds is given by

$$\chi = n_\gamma(n_\gamma+1)(\omega_{R-H} - \omega_{\text{obs}})\omega_{\text{obs}}. \quad (8)$$

The observed speeds (from table 1), Rossby-Haurwitz speeds, and the corresponding values of χ are listed in table 1.

It is immediately obvious that the values for χ are very variable. They are, however, mostly much less than 30, corresponding to Cressman's value of 4 for his factor μ . In general, though with conspicuous exceptions, they can be considered roughly equal to the value of 5 deduced by Rossby and collaborators [12] as appropriate to their free-surface model of the atmosphere. The results do not fit the free-surface model in two ways, however; firstly there is a consistent increase (for the well-defined values) of χ

with decreasing scale, and secondly, in some cases the waves move toward the east although the Rossby-Haurwitz wave-speed is westward. The values of χ are larger in winter or negative, which is consistent with the observation that the summer-winter differences in wave-speed are greater than can be explained by the difference in zonal wind.

The discrepancy of sign of observed and Rossby-Haurwitz speeds is immediately removed if we re-define the barotropic divergence term in equation (6) so that the local derivative $\partial z/\partial t$ refers to a coordinate system moving with the mean zonal wind. This is a straightforward procedure.

4. PREDICTION OF TRAVELING PLANETARY-SCALE WAVES

PREDICTION BASED ON PREVIOUS CHANGES

We have already calculated the fractional reduction in variance of each day's change that can be obtained by estimating it by the linear regression on the previous day's change. It is equal to the square of the vector correlation coefficient, and is tabulated for each wave as R_p^2 in table 1. These values correspond to a skill score for prediction, since they give the fractional reduction of mean square error of the geopotential height compared to holding the wave constant, exact prediction of the particular wave corresponding to 100 percent. Similarly for prediction based on the previous day's change and that of another "adjacent" wave; the corresponding ratios are given in table 4. It should be mentioned that these ratios are necessarily higher than would be achieved if the

regression coefficients were used with an independent sample as in a realistic prediction situation. How much higher depends on the stability of the regression coefficients which needs to be determined from a larger sample than we have considered here.

As would be expected, the ratios in table 4 are larger than those in table 1, but they are in no case much higher; the addition of another wave as a predictor does not produce any significant improvement.

The results must be considered somewhat disappointing as regards practical prediction of these waves. Only Z_2^1 's behavior in summer is regular enough for more than 50 percent of its variance to be accounted for. In summer, results for many of the other harmonics fall in the 20-35 percent range, which may or may not be useful. In winter only the largest-scale wave has more than 30 percent of its variance explained by the regression.

PREDICTION USING THE BAROTROPIC VORTICITY EQUATION

We have computed the vector regression of the observed changes on "predicted" changes calculated from the spherical vorticity equation (7) with values of χ ranging from 0 to 24. The predicted changes were calculated for simple Rossby-Haurwitz waves and using the non-linear vorticity equation including interactions with wave-numbers up to longitudinal wave-number 6. The restriction to long-wave interactions was mainly because of limitations on computer storage, but also because the interactions with the other long waves are the most important ones for the planetary-scale waves (see Eliassen and Machenhauer [7]). The results of these regressions are given in table 5.

TABLE 5.—Correlations of changes with those predicted by spherical vorticity equation, for different values of divergence factor χ . $\overline{\Delta\theta}$ is angle corresponding to regression tensor

	January-February							July-August						
	χ	Rossby-Haurwitz			Non-linear			χ	Rossby-Haurwitz			Non-linear		
		R_p	R_p^2	$\overline{\Delta\theta}$	R_p	R_p^2	$\overline{\Delta\theta}$		R_p	R_p^2	$\overline{\Delta\theta}$	R_p	R_p^2	$\overline{\Delta\theta}$
Z_2^1	0	0.58	0.34	+21°	0.55	0.30	+26°	0	0.78	0.61	+19°	0.78	0.61	+19°
	6	.58	.34	-9°	.55	.30	-3°	6	.78	.61	-10°	.78	-----	-11°
	18	.58	.34	-25°	.55	.30	-18°	18	.78	.61	-24°	.78	-----	-26°
Z_4^1	0	.54	.29	-11°	.56	.31	-6°	0	.46	.21	-17°	.42	.18	-24°
	6	.54	.29	-14°	.56	.31	-8°	6	.46	.21	-21°	.42	.18	-27°
Z_3^2	0	.45	.20	-15°	.42	.18	-12°	0	.66	.44	+15°	.52	.27	+15°
	6	.45	.20	-36°	.42	.18	-36°	6	.66	.44	-4°	.52	.27	-3°
Z_5^2	0	.35	.12	-48°	.30	.09	-39°	0	.52	.27	0°	.50	.25	+2°
	12	.35	.12	-54°	.30	.09	-44°	12	.52	.27	-8°	.50	.25	-7°
Z_4^3	0	.39	.15	-38°	.31	.10	-33°	0	.66	.44	+10°	.66	.44	+9°
	6	.39	.15	-46°	.31	.10	-41°	6	.66	.44	-5°	.66	.44	-8°
Z_6^3	0	.49	.24	-74°	.26	.07	-126°	0	.42	.18	-15°	.42	.18	-15°
	12	.49	.24	-77°	.26	.07	-127°	12	.42	.18	-19°	.42	.18	-19°

REFERENCES

1. T. W. Anderson, *An Introduction to Multivariate Statistical Analysis*, John Wiley and Sons, New York, 1958, 374 pp.
2. J. G. Charney, "The Dynamics of Long Waves in a Baroclinic Westerly Current," *Journal of Meteorology*, vol. 4, No. 5, Oct. 1947, pp. 135-162.
3. G. P. Cressman, "Barotropic Divergence and Very Long Atmospheric Waves," *Monthly Weather Review*, vol. 86, No. 8, Aug. 1958, pp. 293-297.
4. R. J. Deland, "Traveling Planetary-Waves," *Tellus*, vol. 16, No. 2, May 1964, pp. 271-273.
5. R. J. Deland, "Some Observations of the Behavior of Spherical Harmonic Waves," *Monthly Weather Review*, vol. 93, No. 5, May 1965, pp. 307-312.
6. R. J. Deland, "On the Scale Analysis of Traveling Planetary-Waves," *Tellus*, vol. 17, No. 4, Nov. 1965, pp. 527-528.
7. E. Eliassen and B. Machenhauer, "A Study of the Fluctuations of the Atmospheric Planetary Flow Patterns," *Tellus*, vol. 17, No. 2, May 1965, pp. 220-238.
8. T. H. Ellison, "On the Correlation of Vectors," *Quarterly Journal of the Royal Meteorological Society*, vol. 80, No. 343, Jan. 1955, pp. 93-96.
9. B. Haurwitz, "The Motion of Atmospheric Disturbances on a Spherical Earth," *Journal of Marine Research*, vol. 3, No. 3, Dec. 1940, pp. 254-267.
10. R. W. Lenhart, Jr., A. Court, and H. Salmela, "Variability Shown by Hourly Wind Soundings," *Journal of Applied Meteorology*, vol. 2, No. 1, Feb. 1963, pp. 99-104.
11. D. E. Martin, "An Investigation of the Systematic Errors in the Barotropic Forecasts," *Tellus*, vol. 10, No. 4, Nov. 1958, pp. 451-465.
12. C.-G. Rossby and Collaborators, "Relation Between Variations in the Intensity of the Zonal Circulation of the Atmosphere and the Displacements of the Semi-Permanent Centres of Action," *Journal of Marine Research*, vol. 2, No. 1, June 1939, pp. 38-55.
13. P. M. Wolff, "The Error in Numerical Forecasts Due to Retrogression of Ultra-Long Waves," *Monthly Weather Review*, vol. 86, No. 8, Aug. 1958, pp. 245-250.

[Received November 8, 1965; revised August 15, 1966]